International Journal of Industrial Electronics, Control and Optimization © 2021 IECO
Vol. 4, No. 4, pp. 433-444, Sep(2021)

Reliability-Based Operation in Energy Hubs with Several Energy Networks

Alireza Malekijavan[1], Mehdi Aslinezhad[2,†], and Hamidreza Zaferani[3]

[1,2] Department of Electrical Engineering, Shahid Sattari Aeronautical University of Science and Technology, Tehran, Iran

[3] Department of Electrical Engineering, Tehransar-Sama College, Tehran

ABSTRACT

The paper presents reliability-based operation (RBO) of an energy hub consisting of electric vehicles (EVs) and a combined cooling, heating, power (CCHP) system in electricity, natural gas, and district heating networks. The proposed strategy aims to minimize the total expected operating and reliability costs of the mentioned energy networks as its objective functions. Furthermore, the problem is subject to optimal power flow (OPF) equations, reliability constraints, and a hub energy model including constraints of EV parking lots and CCHP. This strategy has a mixed-integer nonlinear programming (MINLP) model, so MILP will be used to achieve a unique optimal solution in less computational time for the proposed scheme. Moreover, the scheme includes uncertainties of the load, energy price, the demand of EVs, and equipment availability of the given systems, which are modeled using scenario-based stochastic programming (SBSP). Finally, the approach is implemented on a standard test system in the GAMS software environment. Then, according to the numerical results, it is observed that the mentioned outline can achieve optimal operating conditions and high reliability in energy systems if the EVs and CCHPs are optimally managed in the energy hub form.

Article Info

Keywords:
Combined cooling, heating and power system, Electrical vehicle parking lot, Energy hub, Reliability-based operation, Stochastic linear programming

Article History:
Received 2020-10-06
Accepted 2021-01-24

NOMENCLATURE

Indices and sets

e, Ξ_{BC}	Index and set of a bus in the electrical network
g, Ξ_{NG}	Index and set of a node in the natural gas network
h, Ξ_{NH}	Index and set of a node in the district heating network
j	Auxiliary index defined as a bus or a node
l, Ξ_{L}	Index and set of linearization segments in the conventional piecewise linear method
k, Ξ_{K}	Index and set of laterals of the regular polygon
ref	Slack bus
t, Ξ_{ST}	Index and set of simulation time
w, Ξ_{SC}	Index and set of scenarios

Variables

$Cost$	Total expected operation and reliability costs ($)
C^C	Cooling power of CCHP per unit (p.u)
$EENS$	Expected energy not-supplied (MWh or p.u)
E^{EV}	Stored energy in the battery of EVs in the parking lot (p.u)
G^C	Gas power of CCHP (p.u)
G^L	Gas power flowing through the pipeline (p.u)
G^S	Gas power of the natural gas station (p.u)
H^C	Heating power of CCHP (p.u)
H^L	Heating power flowing through the pipeline (p.u)
H^S	Heating power of the heat station (p.u)
P^C, Q^C	Active and reactive power of CCHP (p.u)
$P^{EV,B}$, $P^{EV,L}$	Battery power and active loss of EVs chargers in the parking lot (p.u)
$P^{EV,ch}$, $P^{EV,dech}$	Charging and discharging power of EVs (p.u)

†**Corresponding Author**: M.aslinezhad@ssau.ac.ir.
Tel: +982164032229, University of Science and Technology of Shahid Sattari Aeronautical, Tehran 1384663113, Iran

P^L, Q^L Active and reactive power flowing on distribution line (p.u)

P^{LNS}, G^{LNS}, H^{LNS} Active, gas, and heating power not-supplied (p.u)

P^S, Q^S Active and reactive power of distribution station (p.u)

Q^{EV} Reactive power of chargers of EVs in the parking lot (p.u)

T Temperature (p.u)

V, ΔV, θ Voltage magnitude (p.u), deviation (p.u), and angle (radian)

x Binary variable related to charging/discharging state of EVs in the parking lot

π, $\Delta\pi$ Gas pressure and deviation (p.u)

Constants

AL^E, AL^G, AL^H Incident matrix of buses and lines in the electrical networks, Incident matrix of nodes and pipelines in the natural gas networks, and Incident matrix of nodes and pipelines in the district heating network

a^p, a^q Coefficients of active and reactive power in the calculation equation of losses in chargers of EVs

c, $\dot{m}$ Specific heat capacity of water and mass flow rate of water through a pipeline

CR, DR Charging and discharging rates of EVs in the parking lot (p.u)

E^{Arr}, E^{Dep} Energy of EVs at arrival and departure time (p.u)

g, b Conductance and susceptance of distribution line (p.u)

G^{Cmax} Maximum gas capacity of CCHP (p.u)

G^D Gas demand power (p.u)

G^{Lmax} Maximum gas power allowed to flow through the pipeline (p.u)

G^{Smax} Maximum capacity of the natural gas station (p.u)

H^D Heat demand power (p.u)

H^{Lmax} Maximum heat power allowed to flow through the pipeline (p.u)

HR^C The ratio of cooling power to heating power in CCHP

H^{Smax} Maximum capacity of the heat station (p.u)

P^D, Q^D Active and reactive power demand (p.u)

S^{Cmax} Maximum allowed apparent power of CCHP (p.u)

S^{EVmax} Maximum allowed apparent power of chargers of EVs in the parking lot (p.u)

$sign(\pi_g, \pi_j)$ A constant value, which is 1 if π_g is greater than π_j , else is −1.

S^{Lmax} Maximum apparent power allowed to flow through the distribution line (p.u)

S^{Smax} Maximum capacity of the distribution station (p.u)

T^{min}, T^{max} Minimum and maximum allowed temperature (p.u)

V^{min}, V^{max} Minimum and maximum allowed voltage magnitude (p.u)

$VOLL$ Value of lost load ($/MWh)

η^C Efficiency of CCHP

κ Pipeline constant (p.u)

ν Probability occurrence of the scenario

π^{min}, π^{max} Minimum and maximum allowed pressure (p.u)

ρ^E, ρ^G, ρ^H Price of electrical, gas, and heat energy ($/MWh)

I. INTRODUCTION

Nowadays, authorities and organizations encourage energy consumers to utilize state-of-the-art technologies with low emissions to reduce environmental pollution. One of the most widespread technologies to reach this aim is electric vehicles (EVs), which obtain their kinetic energy from the energy stored in their batteries [1-2]. Moreover, the energy demand of EVs is generally supplied via connection to a power system, especially a distribution network [3]. Thus, it is predicted that the number of EVs available in a power system will increase to supply their power demand. Among the proposed technologies are distributed generations (DGs), which can improve operation indices such as voltage profile, energy loss, and distribution lines overloading [4]. Nevertheless, it should be noted that among various types of DGs, combined cooling, heating, and power (CCHP) systems can widely be used in power systems thanks to their high energy efficiency compared to other DGs [5]. Therefore, it is expected to establish an energy management system (EMS) by coordinating EV parking lots and CCHP systems in the form of energy hubs (in short: hubs) and collaboration of hub operators and energy network operators (ENOs) so as to increase energy efficiency, reach an optimal operation, and enhance reliability in energy networks.

Various research studies have been conducted in the field of hub operation in different energy networks. As stated in [6], hubs are expressed based on wind systems. In this reference, a combination of stochastic modeling and the information gap decision theory (IGDT) has been used to consider uncertainty parameters. It is noteworthy that in the IGDT method, the maximum radius of the uncertainty of parameters is obtained for the optimal solution of the problem. In [7], an economic-cooperative scheduling problem model is considered for energy hubs, in which each hub is considered an energy cooperative center. In [8], the constrained-chance optimization problem model is evaluated for a multi-carrier energy (MCE) system consisting of a hub. Ref. [9] presents a new model of hub that can, firstly, increase the use of clean energy and energy efficiency and achieve the goal of local energy consumption. Secondly, according to the interconnected hub framework, calling is carried out on the

internet of energy. Then, an energy distribution management strategy is designed for the hub using the compatibility theory. Finally, case studies show that the price adjustment mechanism with more than 500 hubs is stable, and the price adjustment tends to be a constant value after 15 times. Also, authors in [10] introduce a risk-constrained energy management strategy for hubs consisting of photovoltaics (PVs), compressed air energy storage (CAES), and demand response program (DRP). In this case, stochastic programming has been employed to model the uncertainty parameters of PVs and the load. Additionally, energy storage and demand response have been used to increase the flexibility of the hub in the presence of PV sources. The optimal bidding model of a hub with its participation in energy markets is stated in [11]. In another study, stochastic dynamic programming (SDP) has been used in [12] for optimal hub operation. In [13], the issue of hub participation in the distribution network based on the DRP is presented. Furthermore, a hub participation model is presented in [14] for electric and heating energy markets based on the price clearing model of the mentioned energies. The large hub operating model has been studied in [15] by considering different models of DRP. Ref. [16] provides the daily energy management model of electrical, heating, and gas microgrids in the presence of a hub. Authors in [17] mention the operation of a hub consisting of EVs and a combined heat and power system (CHP). The proposed scheme uses the capability of controlling the reactive power of CHPs and EVs to improve electrical network indices, such as voltage regulation of electrical buses. Also, in the given scheme, a robust model has been utilized to model the uncertainty parameters of consumption loads and EVs.

Based on the literature, it is observed that most research cases focus on the coordination of DGs and active loads (ALs), such as EVs, energy storage systems (ESSs), and DRP in distribution networks. However, in general, the coordination of EVs and CCHPs has rarely been considered in the literature. Yet, it should be noted that the use of EVs has grown significantly in recent years as it helps reduce air pollution. Moreover, CCHP is expected to have significant future benefits due to the simultaneous production of three energy forms and increased energy efficiency. Therefore, the coordination of these cases in the form of a hub can have suitable benefits for energy networks from economic, operational, reliability, flexibility, and security viewpoints. Above all, general research has focused on the operation of hubs in various energy networks and has evaluated the ability of hubs to improve the operation indices of these networks. Nonetheless, it is worth noting that hubs, which act as a local resource in energy grids, can play a role in improving other grid indices, one of the most important of which is reliability. However, this has less been a case in research on the proposed topic.

To compensate for the research gaps mentioned in this paper, the reliability-based operation (RBO) in electrical, natural gas, and district heating networks is presented as shown in Fig. 1. In the proposed scheme, the hub is intended for the aggregation of EV parking lots and CCHP. The suggested problem also undermines the total expected operating and reliability costs in the mentioned energy networks. This problem is also constrained by the power flow (PF) equations and technical and reliability constraints in the given energy networks, and the hub model, consisting of EV parking lots and CCHP. It is noteworthy that this problem has a mixed-integer nonlinear programming (MINLP) model. Therefore, the solvers of this problem can obtain the local optimal solution at high computation time provided that the final solution of each solvent is different. Hence, to achieve a unique optimal solution in low computation time, the mixed-integer linear programming (MILP) model is used for the proposed scheme in the next step. Furthermore, the introduced outline includes uncertainty in consumption loads, energy prices, EV parameters, and availability of energy grid equipment. Therefore, this paper presents scenario-based stochastic programming (SBSP) for modeling these uncertainty parameters, which is based on a combination of the Monte Carlo simulation (MCS) technique and the Kantorovich method. Contributions of this scheme can be summarized as:

- implementing simultaneous reliability and operation problems in electrical, natural gas, and district heating networks consisting of an energy hub;
- coordinating EV parking lots and CCHP in the form of an energy hub to increase energy efficiency and reduce the operation of batteries and chargers of EVs; and
- improving operation, economic, and reliability indices in energy networks using energy hub as a local energy source.

The paper is organized as follows. In Section II, the RBO model of the hub in energy networks is described. Section III provides a linearized model for the proposed problem. Sections IV and V present the numerical results and conclusions, respectively.

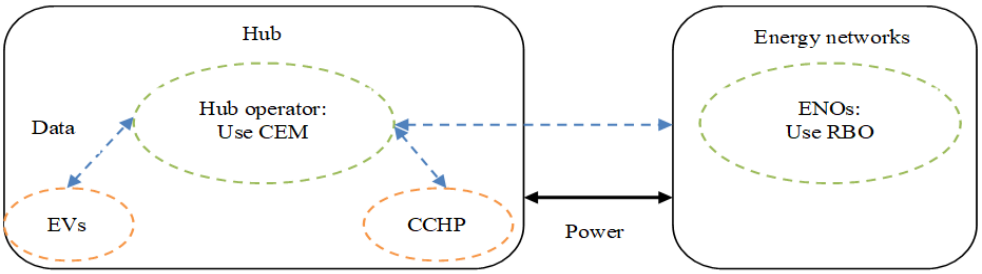

Fig. 1. The suggested scheme for RBO in energy networks in the presence of a hub

II. RBO OF THE HUB IN ENERGY NETWORKS

This section presents the problem of RBO of a hub consisting of an EV parking lot and CCHP in electrical, natural gas, and district heating networks. This minimization problem takes into account the total operating and reliability costs in the proposed networks as the objective function. The problem is also constrained to optimal power flow (OPF) equations, reliability limitation, CCHP equations, and EV parking lot constraints. Therefore, the problem is formulated as follows:

$$\min \quad Cost = \sum_{w\in\Xi_{SC}} \nu_w \sum_{t\in\Xi_{ST}} \left\{ \sum_{e\in\Xi_{BE}} \rho_t^E P_{e,t}^S + \sum_{g\in\Xi_{NG}} \rho^G G_{g,t}^S + \sum_{h\in\Xi_{NH}} \rho^H H_{h,t}^S \right\} + \overbrace{VOLL \times \sum_{w\in\Xi_{SC}} \nu_w \sum_{t\in\Xi_{ST}} \left\{ \sum_{e\in\Xi_{BE}} P_{e,t}^{LNS} + \sum_{g\in\Xi_{NG}} G_{g,t}^{LNS} + \sum_{h\in\Xi_{NH}} H_{h,t}^{LNS} \right\}}^{EENS} \tag{1}$$

Subject to:

$$P_{e.t.w}^{LNS} + P_{e.t.w}^{S} + P_{e.t.w}^{C} + \left(P_{e.t.w}^{EV.dch} - P_{e.t.w}^{EV.ch}\right) - P_{e.t.w}^{D} = \sum_{j\in\Xi_{BE}} AL_{e.j}^{E} P_{e.j.t.w}^{L} \quad \forall e.t.w \tag{2}$$

$$Q_{e.t.w}^{S} + Q_{e.t.w}^{C} + Q_{e.t.w}^{EV} - Q_{e.t.w}^{D} = \sum_{j\in\Xi_{BE}} AL_{e.j}^{E} Q_{e.j.t.w}^{L} \quad \forall e.t.w \tag{3}$$

$$\begin{aligned} P_{e.j.t.w}^{L} = {} & g_{e.j}(V_{e.t.w})^2 \\ & - V_{e.t.w}V_{j.t.w}\{g_{e.j}\cos(\theta_{e.t.w} \\ & - \theta_{j.t.w}) \\ & + b_{e.j}\sin(\theta_{e.t.w} \\ & - \theta_{j.t.w})\} \forall e.j.t.w \end{aligned} \tag{4}$$

$$\begin{aligned} Q_{e.j.t.w}^{L} = {} & -b_{e.j}(V_{e.t.w})^2 \\ & + V_{e.t.w}V_{j.t.w}\{b_{e.j}\cos(\theta_{e.t.w} \\ & - \theta_{j.t.w}) \\ & + g_{e.j}\sin(\theta_{e.t.w} \\ & - \theta_{j.t.w})\} \forall e.j.t.w \end{aligned} \tag{5}$$

$$\theta_{e,t,w} = 0 \qquad \forall e = ref, t, w \tag{6}$$

$$G_{g,t,w}^{LNS} + G_{g,t,w}^{S} - G_{g,t,w}^{D} - G_{g,t,w}^{C} = \sum_{j\in\Xi_{NG}} AL_{g,j}^{G} G_{g,j,t,w}^{L} \qquad \forall g,t,w \tag{7}$$

$$G_{g,j,t,w}^{L} = \kappa_{g,j}\, sign(\pi_{g,t,w}, \pi_{j,t,w}) * \sqrt{sign(\pi_{g,t,w}, \pi_{j,t,w})\left(\pi_{g,t,w}^2 - \pi_{j,t,w}^2\right)} \qquad \forall g,j,t,w \tag{8}$$

$$H_{h,t,w}^{LNS} + H_{h,t,w}^{S} + H_{h,t,w}^{C} - H_{h,t,w}^{D} = \sum_{j\in\Xi_{NH}} AL_{h,j}^{H} H_{h,j,t,w}^{L} \qquad \forall h,t,w \tag{9}$$

$$H_{h,j,t,w}^{L} = c_{h,j}\dot{m}_{h,j}\left(T_{h,t,w} - T_{j,t,w}\right) \qquad \forall h,j,t,w \tag{10}$$

$$V_e^{\min} \le V_{e,t,w} \le V_e^{\max} \qquad \forall e,t,w \tag{11}$$

$$\left(P_{e,j,t,w}^{L}\right)^2 + \left(Q_{e,j,t,w}^{L}\right)^2 \le \left(S_{e,j}^{L\max}\right)^2 \qquad \forall e,j,t,w \tag{12}$$

$$\left(P_{e,t,w}^{S}\right)^2 + \left(Q_{e,t,w}^{S}\right)^2 \le \left(S_{e}^{S\max}\right)^2 \qquad \forall e,t,w \tag{13}$$

$$\pi_g^{\min} \le \pi_{g,t,w} \le \pi_g^{\max} \qquad \forall g,t,w \tag{14}$$

$$-G_{g,j}^{L\max} \le G_{g,j,t,w}^{L} \le G_{g,j}^{L\max} \qquad \forall g,j,t,w \tag{15}$$

$$0 \le G_{g,t,w}^{S} \le G_{g}^{S\max} \qquad \forall g,t,w \tag{16}$$

$$T_h^{\min} \le T_{h,t,w} \le T_h^{\max} \qquad \forall h,t,w \tag{17}$$

$$-H_{h,j}^{L\max} \le H_{h,j,t,w}^{L} \le H_{h,j}^{L\max} \qquad \forall h,j,t,w \tag{18}$$

$$0 \le H_{h,t,w}^{S} \le H_{h}^{S\max} \qquad \forall h,t,w \tag{19}$$

$$0 \le P_{e,t,w}^{LNS} \le P_{e,t,w}^{D} \qquad \forall e,t,w \tag{20}$$

$$0 \le G_{g,t,w}^{LNS} \le G_{g,t,w}^{D} \qquad \forall g,t,w \tag{21}$$

$$0 \le H_{h,t,w}^{LNS} \le H_{h,t,w}^{D} \qquad \forall h,t,w \tag{22}$$

$$0 \le P_{e,t,w}^{EV,dch} \le DR_{e,t,w}x_{e,t} \qquad \forall e,t,w \tag{23}$$

$$0 \le P_{e,t,w}^{EV,ch} \le CR_{e,t,w}\left(1 - x_{e,t}\right) \qquad \forall e,t,w \tag{24}$$

$$P_{e,t,w}^{EV,dch} - P_{e,t,w}^{EV,ch} = P_{e,t,w}^{EV,B} - P_{e,t,w}^{EV,L} \qquad \forall e,t,w \tag{25}$$

$$P_{e,t,w}^{EV,L} = a^p\left(P_{e,t,w}^{EV,dch} + P_{e,t,w}^{EV,ch}\right) + a^q Q_{e,t,w}^{EV} \qquad \forall e,t,w, Q_{e,t,w}^{EV} \ge 0 \tag{26}$$

$$E_{e,t,w}^{EV} = E_{e,t-1,w}^{EV} - P_{e,t,w}^{EV,B} \qquad \forall e,t,w \tag{27}$$

$$E_{e,t,w}^{EV} = E_{e,t,w}^{Arr} \qquad \forall e, t = \text{Arrival time}, w \tag{28}$$

$$E_{e,t,w}^{EV} = E_{e,t,w}^{Dep} \qquad \forall e, t = \text{Departure time}, w \tag{29}$$

$$\left(P_{e,t,w}^{EV,dch} - P_{e,t,w}^{EV,ch}\right)^2 + \left(Q_{e,t,w}^{EV}\right)^2 \le \left(S_{e,t,w}^{EV\max}\right)^2 \qquad \forall e,t,w \tag{30}$$

$$G_{g,t,w}^{C} = \frac{P_{e,t,w}^{C} + H_{h,t,w}^{C} + C_{h,t,w}^{C}}{\eta^c} \qquad \forall g,e,h,t,w \tag{31}$$

$$C_{h,t,w}^{C} = H_{h,t,w}^{C} HR^{C} \qquad \forall h,t,w \tag{32}$$

$$\left(P_{e,t,w}^{C}\right)^2 + \left(Q_{e,t,w}^{C}\right)^2 \le \left(S_{e}^{C\max}\right)^2 \qquad \forall e,t,w \tag{33}$$

$$0 \le G_{g,t,w}^{C} \le G_{g}^{C\max} \qquad \forall g,t,w \tag{34}$$

The objective function has two terms. The first term refers to the expected operation cost of electric, gas, and district heating substations [17], and the reliability cost in electrical, natural gas, and district heating networks is presented in the second term [18]. The reliability cost in the given equation is proportional to the product of the expected energy not supplied (EENS) and the value of lost load (VOLL) [18], in

which case, according to the second term in (1), the EENS is equal to the sum of the electric, gas and, heating loads not supplied on the operation horizon.

Constraints of the problem are given in (2)-(34), in which constraints (2)-(10) are related to PF equations in different energy networks. AC-PF constraints of the power distribution follow (2)-(6). These equations represent the active and reactive power balance at different buses, active and reactive power flowing through the distribution line, and the voltage angle value of the slack bus, respectively [1]. The gas power balance at different nodes and the gas flowing through the pipeline are proportional to constraints (7) and (8), respectively [17]. Moreover, PF equations of district heating network are also presented in constraints (9) and (10), which indicate the heating power balance at different nodes and the heat flowing through the pipeline, respectively [17]. In addition, technical or operational constraints of different energy networks are formulated in (11)-(19). The technical constraints of the electrical network, including the voltage limit of the buses, the limitation of the distribution line, and station capacities, are presented in (11)-(13), respectively [19]. Also, the pressure limit on the nodes and the capacity limit of the pipeline and the gas station in the natural gas network correspond to constraints (14)-(16), respectively. Finally, the limits on the temperature of the nodes, the capacity of the pipeline, and the heating station capacity proportional to the heating network are listed in (17)-(19). Constraints on reliability in electrical, natural gas, and district heating networks are provided in (20)-(22), respectively [18].

Constraints of the hub consisting of an EV parking lot and CCHP are given in (23)-(34). It is noteworthy that in the equations, it is assumed that there is cooling load only in the hub where it is supplied by CCHP. Also, EVs are connected to the network during the day after their last trip [1]. According to these cases, equations (23) to (30) will be equal to the constraints of the EV parking lot, which in turn represent the constraints concerning the charging and discharging rates of the EV batteries in the parking lot, the power balance in the EV parking lot, the calculation of EV charger power losses in the parking lot, the energy stored in the EV batteries in the parking lot, the initial and final energy amounts at the arrival and departure times for the EVs in the parking lot, and the charging capacity limit of the EVs in the parking lot, respectively [1]. It should be noted that the electrical network generally has inductive loads, so it is expected that the EV charger will operate in the capacitive mode. Therefore, the reactive power variable of EVs always has a positive value for (26). Note that in these equations, CR, DR, and S^{EVmax} are equal, to $\sum_{i=1}^{N_t} cr_i$, $\sum_{i=1}^{N_t} dr_i$, and $\sum_{i=1}^{N_t} cc_i$, respectively where cr, dr, and cc represent the charging rate, discharging rate, and charger capacity of an EV, respectively. N_t represents the number of EVs available in the parking lot at time t. Also, the E^{Arr} and E^{Dep} parameters can be calculated from $\sum_{i=1}^{NA} soc_i bc_i$ and $\sum_{i=1}^{ND} bc_i$, respectively in which bc and soc represent the battery capacity and state of charge (SOC) of an EV battery, respectively. NA and ND indicate the number of EVs at arrival and departure times, respectively [1]. Finally, the CCHP constraints are expressed in (31) to (34). The power balance in different parts of the CCHP is proportional to constraint (31). Additionally, the CCHP cooling power is generally a coefficient of its heating power, which is shown in equation (32). Capacity constraints of the CCHP in electrical and gas sectors correspond to (33) and (34), respectively. One should note that since the input limit of the CCHP (gas section) and one of its outputs (electrical section) is taken into account, the constraint of the heating and cooling section can be neglected in the CCHP problem model. Besides, in this case, it is assumed that the CCHP cooling power is consumed in the hub, so the cooling network model is not required in this formulation.

In the suggested problem, load (P^D, Q^D, G^D, and H^D), energy price (ρ^E, ρ^G, and ρ^H), parameters of the EV (CR, DR, S^{EVmax}, E^{Arr}, and E^{Dep}), and availability of energy network equipment such as distribution lines, pipelines, and stations are uncertain. Therefore, the SBSP is utilized in this paper to model these parameters. In this method, first, the MCS generates a high number of scenarios for load and energy prices corresponding to the normal probability distribution function (PDF) for EV parameters proportional to Rayleigh PDF [20], and for accessibility of equipment according to Bernoulli PDF [18]. Then, the Kantorovich method is used as a scenario reduction approach to achieve a lower number of scenarios with a higher probability of occurrence. This method selects scenarios that have a minimum distance to each other, but this statement describes an NP-hard set-covering problem that is too large in scale to be practical in many applications [21]. The Kantorovich method can obtain final scenarios in a shorter time than the other scenario reduction methods. Most details of this approach are described in [21].

III. LINEAR APPROXIMATE MODEL OF THE PROPOSED PROBLEM

The problem model presented in the previous section is an MINLP caused by nonlinear constraints (4), (5), (8), (12), (13), (30), and (33) and non-convex equations (4) and (5) [1, 17]. Since the hub operation problem in different networks is a complicated optimization problem, the solvers of this problem model cannot be expected to achieve a unique solution in low computation time. In other words, different solvers may reach different optimal solutions, impairing reliance on the solutions of these solvers [1]. To overcome this issue, it is recommended to linearize nonlinear equations.

To linearize equations (4) and (5), it should be noted that in a distribution network, in general, bus voltages are close to 1 p.u., so the voltage magnitude will be 1 + ΔV where ΔV denotes the voltage deviation. Furthermore, the voltage angle difference between the two ends of a distribution line is less than 6° (or 0.105 rad). Thus, $\cos\left(\theta_{e,t,w}-\theta_{j,t,w}\right)$ and $\sin\left(\theta_{e,t,w}-\theta_{j,t,w}\right)$ terms can be approximated by 1 and $\left(\theta_{e,t,w}-\theta_{j,t,w}\right)$, respectively. Therefore, linearized forms of constraints (4) and (5) and bus voltage limitations considering the above assumptions and neglecting ΔV^2, $\Delta V_e \Delta V_j$, and $\Delta V \times (\theta_e - \theta_j)$ will be as follows [17]:

$$P^L_{e,j,t,w} = g_{e,j}\left(\Delta V_{e,t,w}-\Delta V_{j,t,w}\right)-b_{e,j}\left(\theta_{e,t,w}-\theta_{j,t,w}\right) \qquad \forall e,j,t,w \tag{35}$$

$$Q^L_{e,j,t,w} = -g_{e,j}\left(\theta_{e,t,w}-\theta_{j,t,w}\right)-b_{e,j}\left(\Delta V_{e,t,w}-\Delta V_{j,t,w}\right) \qquad \forall e,j,t,w \tag{36}$$

$$V_e^{\min}-1 \le \Delta V_{e,t,w} \le V_e^{\max}-1 \qquad \forall e,t,w \tag{37}$$

To linearize (8), it is first rewritten as (38) where the auxiliary variable ξ can be calculated from $\left(\xi_{g,j,t,w}\right)^2 = sign(\pi_{g,t,w},\pi_{j,t,w})\left(\pi^2_{g,t,w}-\pi^2_{j,t,w}\right)$. However, this is a quadratic polynomial nonlinear equation that can be approximated to a linear equation using the conventional piecewise linearization method [1]. Based on this method, variables ξ and π are divided into several variables with a small range of changes, i.e. $\Delta\xi$ and $\Delta\pi$, the sum of which gives the values of ξ and π similar to constraints (39) and (40). Moreover, the square of each variable, such as ξ^2 (π^2), can be expressed as $\sum_{l\in\Xi_L} s^{\xi}_l \Delta\xi_l$ ($\sum_{l\in\Xi_L} s^{\pi}_l \Delta\pi_l$), where l and Ξ_L are the index and the set of linearized segments, and s denotes the piecewise slope. Consequently, the proposed quadratic polynomial equation is linearized as (41).

$$G^L_{g,j,t,w} = \kappa_{g,j}\, sign(\pi_{g,t,w},\pi_{j,t,w})\,\xi_{g,j,t,w} \tag{38}$$

$$\xi_{g,j,t,w} = \sum_{l\in\Xi_L}\Delta\xi_{g,j,t,w,l} \qquad \forall g,j,t,w \tag{39}$$

$$\pi_{g,t,w} = \pi_g^{\min} + \sum_{l\in\Xi_L}\Delta\pi_{g,t,w,l} \qquad \forall g,t,w \tag{40}$$

$$\sum_{l\in\Xi_L} S^{\xi}_l \Delta\xi_{g.j.t.w.l} = sign(\pi_{g.t.w}.\pi_{j.t.w})\left(\sum_{l\in\Xi_L} S^{\pi}_l(\Delta\pi_{g.t.w.l} - \Delta\pi_{j.t.w.l})\right) \forall g.j.t.w \tag{41}$$

Constraints (12), (13), (30), and (33) are in the form of a circular plane with a radius of S, i.e., $P^2+Q^2 \le S^2$. The plane can be approximated by a regular polygon [1] such that if the number of laterals is high, a more accurate approximation is reached. It is noted that the laterals of this regular polygon correspond to a straight line in the form of $P\times\cos\left(k\times\Delta\beta\right)+Q\times\sin\left(k\times\Delta\beta\right)=S$ where $\Delta\beta$ is the angle deviation equal to $360/n_k$ in which n_k represents the number of laterals of the regular polygon, and k is the index of linearization segments, which varies between 0 and $n_k - 1$ in set Ξ_k. Finally, the proposed regular polygon plane is the overlaps of planes $P\times\cos\left(k\times\Delta\beta\right)+Q\times\sin\left(k\times\Delta\beta\right)\le S$ if this equation is repeated for all values of k. Therefore, the linearized equations of constraints (12), (13), (30), and (33) are rewritten as:

$$P^L_{e,j,t,w}\cos\left(k\times\Delta\beta\right)+Q^L_{e,j,t,w}\sin\left(k\times\Delta\beta\right)\le S^{L\max}_{e,j} \qquad \forall e,j,t,w,k \tag{42}$$

$$P^S_{e,t,w}\cos\left(k\times\Delta\beta\right)+Q^S_{e,t,w}\sin\left(k\times\Delta\beta\right)\le S^{S\max}_{e} \qquad \forall e,t,w,k \tag{43}$$

$$\left(P^{EV,dch}_{e,t,w}-P^{EV,ch}_{e,t,w}\right)\cos\left(k\times\Delta\beta\right)+Q^{EV}_{e,t,w}\sin\left(k\times\Delta\beta\right)\le S^{EV\max}_{e,t,w} \qquad \forall e,t,w,k \tag{44}$$

$$P^C_{e,t,w}\cos\left(k\times\Delta\beta\right)+Q^C_{e,t,w}\sin\left(k\times\Delta\beta\right)\le S^{C\max}_{e} \qquad \forall e,t,w,k \tag{45}$$

As a result, the suggested linearized problem model in the form of an MILP that can be solved using conventional solvers such as CPLEX is as follows:

$$\min \quad Cost = \sum_{w\in\Xi_{SC}} \nu_w \sum_{t\in\Xi_{ST}} \left\{ \sum_{e\in\Xi_{BE}} \rho^E_t P^S_{e,t} + \sum_{g\in\Xi_{NG}} \rho^G G^S_{g,t} + \sum_{h\in\Xi_{NH}} \rho^H H^S_{h,t} \right\} + \overbrace{VOLL\times \sum_{w\in\Xi_{SC}} \nu_w \sum_{t\in\Xi_{ST}} \left\{ \sum_{e\in\Xi_{BE}} P^{LNS}_{e,t} + \sum_{g\in\Xi_{NG}} G^{LNS}_{g,t} + \sum_{h\in\Xi_{NH}} H^{LNS}_{h,t} \right\}}^{EENS} \tag{46}$$

Subject to:

Constraints (2), (3), (6), (7), (9), (10), (14)-(29), (31), (32), (34)-(45) (47)

IV. NUMERICAL RESULTS

4.1. Data

The proposed problem is applied to a system consisting of a 9-bus electric grid, a 4-node natural gas system, and a 7-node district heating network as shown in Fig. 2 [17]. The base values of power, voltage, pressure, and temperature in the given system are 1 MW, 1 kV, 10 bar, and 100°C, respectively, and the allowable range of voltage, pressure, and temperature is equal to [0.9, 1.1] p.u. The specifications of the distribution lines, pipelines, stations, and electrical loads are selected from [17]. Also, the daily curve of electricity, gas, and heating energy prices is illustrated in Fig. 3. In addition, the proposed system includes 7 hubs, the position of which is shown in Fig. 2. Each of the hubs, other than Hub 4, has 200 EVs, with the EV penetration level curve given in Fig. 4 [22], and other EV specifications such as charging/discharging rates, SOC, battery capacity, charger capacity, and more are proportional to the data selected from [1, 22]. Hubs 4, 6, and 7 have a CCHP with specifications as follows. The capacity of the input gas and the output electricity is 2.5 MW and 1 MW, respectively, the efficiency

ηc is 0.8, and it is assumed that 20% of its output heat capacity is used to cool the hub. In this section, the

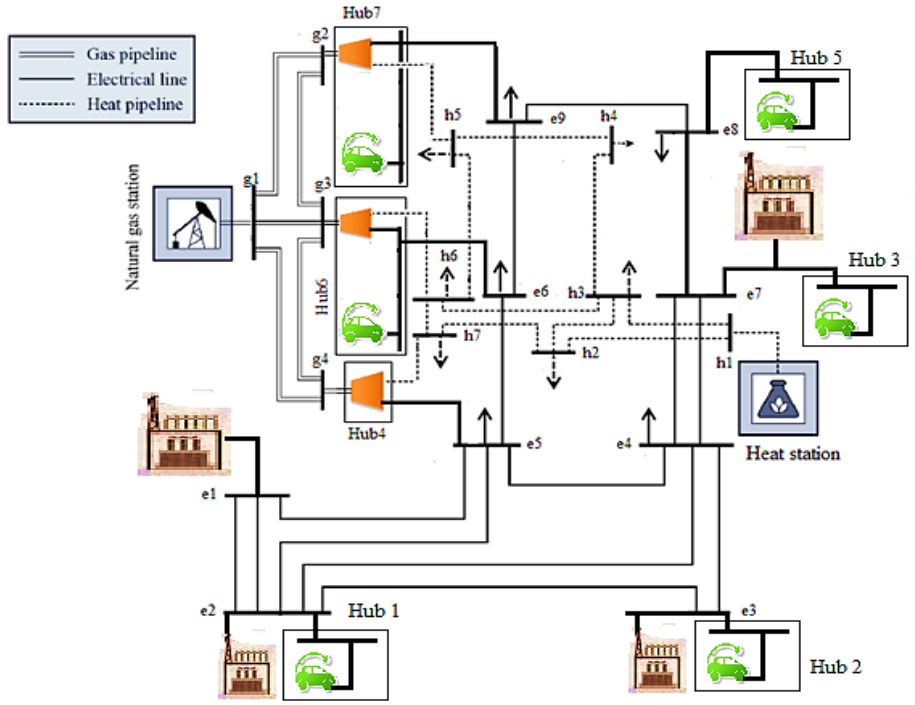

Fig. 2. The studied system [17]

standard deviation for uncertainties of load, energy price, and EV parameters is set at 10%. Regarding the uncertainty of accessibility of network equipment, this parameter depends on the forced outage rate (FOR), the amount of which is assumed to be 1% for all electrical network equipment and 0.5% for the equipment of other networks. Finally, the MCS generates 1000 scenarios for the mentioned uncertainties, and then the Kantorovich method selects 40 scenarios with a high probability of occurrence.

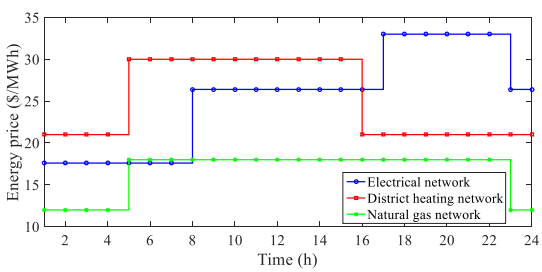

Fig. 3. The daily curve of energy price in different networks

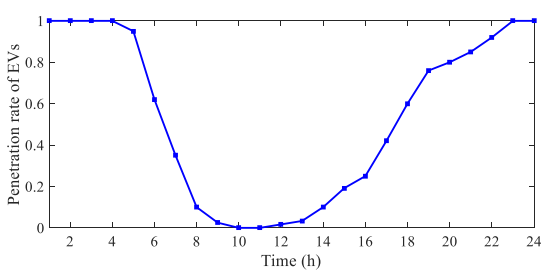

Fig. 4. The daily curve of EV penetration level [22]

4.2. Results

The problem is coded in the GAMS software environment and the CPLEX solver is then used to achieve the optimal solution [23].

A) The capability of the proposed linear model: In this section, it is assumed that the number of pieces in the conventional piecewise linear method is equal to 5, and also the circular plane is approximated by a regular 45-gon. The results of this section are presented in Table I. Accordingly, the solvers of the MINLP model, such as BONMIN, BARON, and KNITRO, produce different solutions for the proposed problem, where BONMIN can achieve a better solution (including lower result for the objective function and calculation time) versus other MINLP solvers. However, MILP solvers such as CPLEX, CBC, and CONOPT can achieve unique optimal solutions with the lowest calculation time in comparison to MINLP solvers. Based on Table I, it is observed that the computational error for active and reactive power is about 2.2%, and this value is about 0.5% for voltage. The computational error for the variables of gas and heat networks is very low; its value for gas power, pressure, heat power, and temperature is about 0.7%, 0.1%, and 0%, respectively.

TABLE I

RESULTS OF THE PROPOSED MILP AND MINLP MODELS

Results of different solvers			
Model	Solver	Cost ($)	Calculation time (s)
MINLP	BONMIN	5768.25	791.67
	BARON	6311.42	1023.22
	KNITRO	Infeasible	-
MILP	CPLEX	5399.13	12.31
	CBC	5399.13	15.78
	CONOPT	5399.13	18.92

Parameter	MINLP	MILP	Percentage of deviation
Solver	BONMIN	CPLEX	-
The sum of the expected active power of distribution stations in the operation horizon (p.u)	82.5451	82.4278	2.23
The sum of the expected reactive power of distribution stations in the operation horizon (p.u)	54.9965	56.2448	2.19
The sum of the expected gas power of gas stations in the operation horizon (p.u)	77.3520	76.8143	0.7
The sum of the expected heat power of heat stations in the operation horizon (p.u)	43.7935	43.7935	0
Average voltage magnitude (p.u)	0.9816	0.9765	-0.52
Average voltage angle (rad)	0.004034	0.004016	-0.448
Average pressure (p.u)	0.9290	0.9281	-0.1
Average temperature (p.u)	0.9347	0.9347	0
Computation time	791.67	12.31	-

TABLE II

The Expected Operation and Reliability Cost in Energy Networks for Different Case Studies

Energy management system		Expected operation cost ($)	Expected reliability cost ($)	Total cost ($)
UEM	EVs	6211.47	1612.31	7823.78
	CCHP	5783.43	1246.22	7029.65
CEM		4857.49	541.64	5399.13

TABLE III

Expected Values of Operation Indices in Different Energy Networks for Different Case Studies

Case	Energy loss (p.u) in the network of			Maximum deviation (p.u) of		
	Electrical	Gas	Heating	Voltage	Pressure	Temperature
I	4.1	0	2.1	0.103	0	0.112
II	3.8	0	2.1	0.086	0	0.112
III	2.7	1.7	1.4	0.053	0.086	0.074
IV	2.4	1.8	1.4	0.047	0.086	0.074

This indicates that the proposed MILP model has a very low computational error compared to the original MINLP model. It is also noteworthy that according to Table I, the computation time in the MILP model by the CPLEX solver is 12.31 s, while in the MINLP model, it is 791.67 s. This also proves the feasibility of the proposed problem in achieving the optimal solution in the shortest possible time. Therefore, according to the stated cases, the proposed MILP model will be a suitable alternative to the original MINLP model.

B) *Evaluating the coordination compatibility of the EV parking lot and CCHP in the form of a hub*: This section examines the coordination compatibility of the EV parking lot and CCHP in the form of a hub. To this end, two strategies have been performed. The first strategy focuses on the uncoordinated energy management (UEM) of these resources. In other words, in this strategy, the operation of energy networks has been carried out for only EV parking lot (the first case study) or CCHP (the second case study) as two separate problems. The second strategy is a coordinated energy management (CEM) plan that uses a hub form to coordinate the EV parking lot and CCHP. The results of this section are tabulated in Table II. Based on this, it is observed that the operation of different networks in the presence of only the EV parking lot has high operation and reliability costs, i.e., 6211.47$ and 1612.31$, compared to the other study case with UEM. In the case of the second study, the operation and reliability

costs decrease by about 6.9% and 22.7%, respectively, compared to the first case study because only the CCHP is responsible for energy production in this case. Nevertheless, in the first case study, EVs are in the form of active loads that, besides controlling network indices, must receive high energy to their travel in a day. However, it should be noted that in the CEM strategy, the energy hub has been able to reduce the operation and reliability cost to a large extent compared to the case studies of the first strategy such that it has reduced the operation (reliability) cost of energy networks by about 16% (56.5%) compared to the second case study in the first strategy. This indicates the ability of the energy hub as a framework for coordinated energy management between different sources and active loads in improving the economic costs of different energy networks.

Figs. 5 to 7 show the daily power injection curve of the hubs to different energy networks. The daily curves of their active and reactive power are shown in Fig. 5. Based on Fig. 5(a), it is observed that the hubs receive active power from 1:00 to 7:00 and 13:00 to 15:00 from the electrical network, but at other times, they can inject power into the network. This is due to the operation of the EV parking lot and CCHP as follows:

- EVs perform charging operations and receive a high amount of power from the network to minimize the operation cost of the electrical network and their own charging cost from 1:00 to 7:00 when the electricity price is the lowest based on Fig. 3. They also perform recharging operations from 12:00 to 16:00, when the charged energy level during these hours is low due to the low number of EVs connected to the electrical grid, as given in Fig. 4. The EVs then inject their stored energy into the network to improve operation indices such as voltage profiles and reduce electrical losses during peak hours, i.e., from 17:00 to 22:00, which correspond to high electrical energy price based on Fig. 3. This amount of energy is low because a low number of EVs have been able to perform the charging operation between 12:00 and 16:00, and it is also supposed that the initial energy of the EVs is low at the moment of connection to the network.
- CCHPs generally have four levels of produced active power based on Fig. 5(a). At the first level, from 5:00 to 7:00, they produce almost no power. From 8:00 to 15:00, according to the second level, they produce an active power of roughly 0.25 p.u. At the third level, they produce an active power of about 0.9 p.u. from 1:00 to 4:00. Finally, at the fourth level corresponding to 16:00-24:00, CCHPs generate an active power of about 1.8 p.u. At the first level, since the price of gas energy based on Fig. 3 is higher than the electricity price, according to Eq. (1), CCHPs are not inclined to produce active power to minimize the operation cost of the electrical network. At the second level, the price of heat energy has the highest value based on Fig. 3; hence, CCHPs are more inclined to produce heat, while producing less active power. In the third and fourth levels, the difference between electricity and gas prices has a positive value, so that this value is high for the fourth level. Therefore, CCHPs produce high power at the fourth level.

The daily curve of the reactive power of the hubs and their elements are presented in Fig. 5(b). It is observed that EVs produce high reactive power from 1:00 to 7:00 because, during these hours, the EVs receive a high level of active power from the network, referring to Fig. 5(a). Hence, it is predicted that if the reactive power of the hubs is not managed, bus voltages will drop sharply. Therefore, EVs and CCHPs generate high reactive power at these hours to regulate the voltage buses, so the hubs inject high reactive power into the network during these hours. At other times, CCHPs can maintain the bus voltages within their allowable range of 0.9 to 1.1 p.u. Also, since EVs based on Eq. (26) inject reactive power into the grid and increase charger losses and operation costs, it is not cost-effective to utilize reactive power in these situations. So, between 8:00 and 24:00, EVs do not generate reactive power. Finally, during these hours, the reactive power curve of the hubs will be equal to the reactive power curve of the CCHPs. Note that this indicates the advantage of coordination between EVs and CCHPs in the form of a hub such that if only EVs were present in the network, higher operation costs would have to be paid to manage the reactive power of the electrical network.

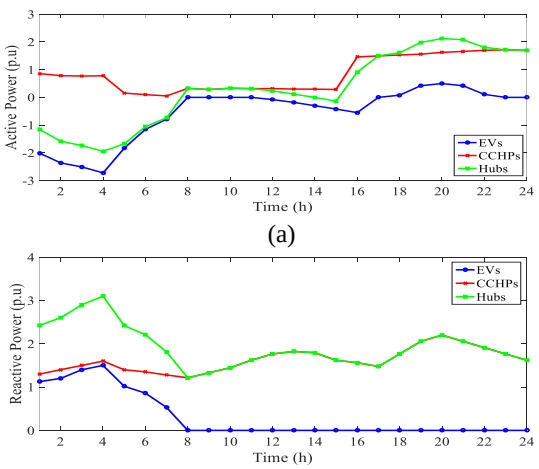

Fig. 5. The daily curve of hubs and their elements, (a) active power, and (b) reactive power

As is seen in Fig. 6, hubs inject higher amounts of heat power into the district heating network from 8:00 to 15:00, compared to other hours because, in these hours, the difference between heat and gas energy prices is higher than that between electrical and gas energy prices, as Fig. 3 presents. Consequently, CCHPs and/or hubs are more inclined to generate higher heat power. However, the contrary is true from 16:00 to 24:00. As a result, CCHPs are more inclined to generate active power (Fig. 5(a)), so their heat power will be lower during these hours. From 1:00 to 4:00, the heat power level, as shown in Fig. 6, is proportional to the ratio of the difference between heat and gas energy prices (22 – 12 = 10 $/MWh) to the difference between the electrical and gas energy prices (17.6 – 12 = 5.6 $/MWh). Finally, the daily gas power curve of hubs will be as Fig. 7, where its value is constant during all hours. This is due to the operation of CCHPs in electrical and heat sectors in proportion to Figs. 5 and 6.

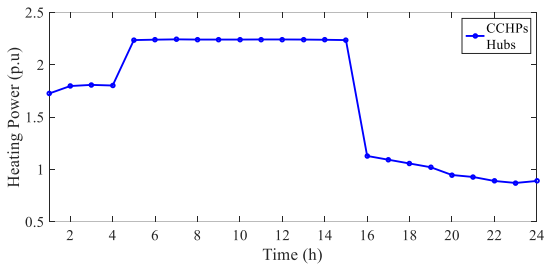

Fig. 6. The daily heat power curve of all hubs

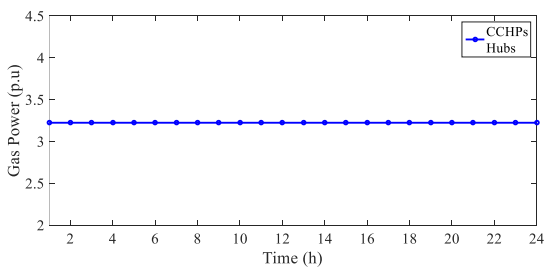

Fig. 7. The daily gas power curve of all hubs

C) Evaluation of capabilities of energy hub in energy networks: The results of the operation indicators of energy networks are listed in Table III in accordance with four different study cases, the details of which are as follows:

- Case I: Power flow analysis neglecting the hubs
- Case II: Proposed problem considering EVs only
- Case III: Proposed problem considering CCHPs only
- Case IV: Proposed problem considering hubs

Table III shows that electrical and heat energy losses in the first study have the highest values, namely, 4.1 and 2.1 p.u, compared to other case studies, respectively. This is also true for the maximum voltage and temperature deviation (maximum value of voltage or temperature deviation from 1p.u). Adding EVs to the first case study (Case II) reduces these indices, but the rate of decline is very low because EVs operate as active loads that have a higher consumption rate than their generation, referring to Fig. 5. Nevertheless, the addition of CCHPs to power grids (Case III) improves or reduces these indices to a high degree compared to Case II. Yet, in this case study, about 1.7 p.u gas energy loss appears and the maximum pressure deviation from zero increases to 0.086 p.u in Case I. Finally, in Case IV, which considers the hub, electrical and heat energy losses are reduced by about 41.5% and 33% compared to Case I, respectively. This reduction for maximum voltage and temperature deviations is about 54.3% and 33%, respectively. These features are created for the proposed strategy by causing 1.8 p.u gas energy loss and a maximum of 0.086 p.u pressure deviation.

The results of reliability in energy networks are proportional to Figs. 8 and 9. Fig. 8 evaluates the EENS changes for the VOLL variations. One can observe that increasing VOLL reduces EENS, until in VOLL of more than 80 $/MWh, the amount of EENS will be constant and equal to 5.41 p.u. In addition, Fig. 9 illustrates the expected operation and reliability cost changes in terms of the VOLL. As can be seen in this figure, an increase in VOLL increases the operation cost, while for a VOLL value of higher than 80 $/MWh, it is fixed at 4857.49$ because, in these conditions, the amount of EENS based on Fig. 8 has a constant value. The expected reliability cost in VOLL is 20 $/MWh, which has the highest value according to the EENS value in Fig. 8, but in other VOLL values, its value decreases. Additionally, although in the VOLL values of more than 80 $/MWh, the expected operation cost and EENS have fixed values, the expected reliability cost increases with increasing VOLL because the cost, based on Eq. (1), is equal to the product of EENS and VOLL.

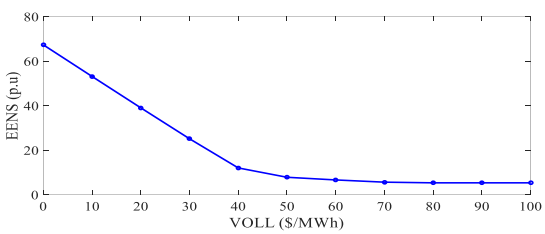

Fig. 8. The EENS curve in terms of VOLL

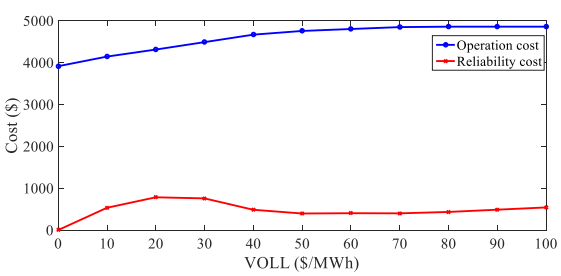

Fig. 9. Expected operation and reliability cost curve in terms of VOLL

V. CONCLUSIONS

The paper presented an RBO of hubs in electrical, natural gas, and district heating networks, where the hub is a framework for coordinating EV parking lots and CCHP. The problem considers the total expected operation and reliability costs of the energy networks provided that OPF constraints, the reliability limitation, and the constraints of the hub with EV parking lots and CCHP are taken into account in these networks. Then, the linearized model of the proposed scheme was employed to determine the optimal solution. Moreover, the SBSP method was utilized to model the uncertainty of the load, energy price, EV parameters, and accessibility of network equipment. Finally, considering the numerical results, it was observed that the linearized problem model was able to obtain the unique optimal solution with a maximum computational error of 2.2% in a very short time compared to the main model of the problem. Furthermore, a coordinated energy management plan between EVs and CCHP in the form of a hub can reduce the operation and reliability cost by about 16% and 56.5%, respectively, compared to the uncoordinated energy management plan. Besides, the hub uses those resources with lower operating costs to manage power. Finally, considering the VOLL equal to 80 $/MWh for the given study system, energy networks with high reliability can be achieved.

REFERENCES

[1] S. Pirouzi, M.A. Latify, G.R. Yousefi, "Conjugate active and reactive power management in a smart distribution network through electric vehicles: A mixed integer-linear programming model," *Sustainable Energy*, Grids and Networks, (accepted), 2020.

[2] M. Ramzanzadeh, and et al. "Security-Constrained Unit Commitment in the Presence of Demand Response Programs and Electric Vehicles," *International Journal of Industrial Electronics*, Control and Optimization, vol. 3, no. 3, pp. 313-326, 2020.

[3] S. Pirouzi *et al*., "Power Conditioning of Distribution Networks via Single-Phase Electric Vehicles Equipped," *IEEE Systems Journal*, vol. 13, no. 3, pp. 3433-3442, 2019.

[4] Q. Zhou, Z. Tian, M. Shahidehpour, X. Liu, A. Alabdulwahab and A. Abusorrah, "Optimal Consensus-Based Distributed Control Strategy for Coordinated Operation of Networked Microgrids," *IEEE Transactions on Power Systems*, vol. 35, no. 3, pp. 2452-2462, 2020.

[5] F. Zhao, C. Zhang and B. Sun, "Initiative optimization operation strategy and multi-objective energy management method for combined cooling heating and power," *IEEE/CAA Journal of Automatica Sinica*, vol. 3, no. 4, pp. 385-393, 2016.

[6] A. Dolatabadi, M. Jadidbonab and B. Mohammadi-ivatloo, "Short-Term Scheduling Strategy for Wind-Based Energy Hub: A Hybrid Stochastic/IGDT Approach," *IEEE Transactions on Sustainable Energy*, vol. 10, no. 1, pp. 438-448, 2019.

[7] S. Fan, Z. Li, J. Wang, L. Piao and Q. Ai, "Cooperative Economic Scheduling for Multiple Energy Hubs: A Bargaining Game Theoretic Perspective," *IEEE Access*, vol. 6, pp. 27777-27789, 2018.

[8] D. Huo, C. Gu, K. Ma, W. Wei, Y. Xiang and S. Le Blond, "Chance-Constrained Optimization for Multienergy Hub Systems in a Smart City," *IEEE Transactions on Industrial Electronics*, vol. 66, no. 2, pp. 1402-1412, 2019.

[9] Y. Yu, T. Zhang, Y. Du and Q. Shao, "Energy hub model for energy management in energy internet," *The Journal of Engineering*, vol. 2019, no. 9, pp. 5432-5438, 2019.

[10] M. Jadidbonab, A. Dolatabadi, B. Mohammadi-Ivatloo, M. Abapour and S. Asadi, "Risk-constrained energy management of PV integrated smart energy hub in the presence of demand response program and compressed air energy storage," *IET Renewable Power Generation*, vol. 13, no. 6, pp. 998-1008, 2019.

[11] T. Zhao, X. Pan, S. Yao, C. Ju and L. Li, "Strategic Bidding of Hybrid AC/DC Microgrid Embedded Energy Hubs: A Two-Stage Chance Constrained Stochastic Programming Approach," *IEEE Transactions on Sustainable Energy*, vol. 11, no. 1, pp. 116-125, 2020.

[12] S. Moazeni, A. H. Miragha and B. Defourny, "A Risk-Averse Stochastic Dynamic Programming Approach to Energy Hub Optimal Dispatch," *IEEE Transactions on Power Systems*, vol. 34, no. 3, pp. 2169-2178, 2019.

[13] M. Majidi and K. Zare, "Integration of Smart Energy Hubs in Distribution Networks Under Uncertainties and Demand Response Concept," *IEEE Transactions on Power Systems*, vol. 34, no. 1, pp. 566-574, 2019.

[14] R. Li, W. Wei, S. Mei, Q. Hu and Q. Wu, "Participation of an Energy Hub in Electricity and Heat Distribution Markets: An MPEC Approach," *IEEE Transactions on Smart Grid*, vol. 10, no. 4, pp. 3641-3653, 2019.

[15] D. Zhang and T. Liu, "A Multi-Step Modeling and Optimal Operation Calculation Method for Large-Scale Energy Hub Model Considering Two Types Demand Responses," *IEEE Transactions on Smart Grid*, vol. 10, no. 6, pp. 6735-6746, 2019.

[16] H. Reza Massrur, T. Niknam and M. Fotuhi-Firuzabad, "Day-ahead energy management framework for a networked gas–heat–electricity microgrid," *IET Generation, Transmission & Distribution*, vol. 13, no. 20, pp. 4617-4629, 2019.

[17] H.R. Zafarani, S.A. Taher, M. Shahidehpour, "Robust operation of a multicarrier energy system considering EVs and CHP units," *Energy*, vol. 192, pp.1-12, 2020.

[18] H.R. Hamidpour, J. Aghaei, S. Pirouzi, S. Dehghan, T. Niknam, "Flexible, reliable, and renewable power system resource expansion planning considering energy storage systems and demand response programs," *IET Renewable Power Generation*, vol. 13, no. 11, pp. 1862-1892, 2019.

[19] M.A. Norouzi, J. Aghaei, S. Pirouzi, T. Niknam, M. Lehtonen, "Flexible operation of grid-connected microgrid using ES," *IET Generation, Transmission & Distribution*, (accepted), 2020.

[20] B. Khorramdel, H. Khorramdel, and J. Aghaei., "Voltage security considerations in optimal operation of BEVs/PHEVs integrated microgrids," *IEEE Trans on Smart Grid.*, vol. 26, no. 2, pp. 12-23, 2014.

[21] J. Aghaei, M. Barani, M. Shafie-khah, A.A.S.d.l. Nieta, and J.P.S. Catalão, "Risk-constrained offering strategy for aggregated hybrid power plant including wind power producer and demand response provider," *IEEE*

Transactions on Sustainable Energy, vol. 7, no. 2, pp. 513-525, 2016.
[22] S. Pirouzi, J. Aghaei, T. Niknam, H. Farahmand, M. Korpås, "Exploring prospective benefits of electric vehicles for optimal energy conditioning in distribution networks," *Energy*, vol. 157, pp. 679-689, 2018.
[23] Generalized algebraic modeling systems (GAMS). [Online]. Available: http://www.gams.com.

Alireza Malekijavan received his B.Sc. degree from the Shahid Sattari Aeronautical University of Science and Technology, Iran, and his M.Sc. degree from Khajenasir, Tehran, Iran, and his Ph.D. degree from Khajenasir University, Tehran, Iran. His current research interests include high-frequency circuit design and intelligent signal processing.

Mehdi Aslinezhad received his B.Sc. degree from the Shahid Sattari Aeronautical University of Science and Technology, Iran in 2003, his M.Sc. degree from Islamic Azad University, Tehran, Iran in 2010, and his Ph.D. degree from Kashan University, Iran in 2019. His current research interests are turbine monitoring, transformer monitoring, and sensors.

Hamidreza Zafarani received his B.Sc. and M.Sc. degrees from Islamic Azad University, Tehran, Iran in 2010 and his Ph.D. degree from Kashan University, Iran in 2020. His current research interests include the application of power electronics in renewable energy systems and electrified railway systems, restructured market, distributed generation, smart grid, electrical vehicles, reactive power control, power quality management, and compensation systems such as SVC, UPQC, FACTS devices.